NACA TN 3978

NATIONAL ADVISORY COMMITTEE FOR AERONAUTICS

TECHNICAL NOTE 3978

SURVEY OF THE ACOUSTIC NEAR FIELD OF THREE NOZZLES AT A PRESSURE RATIO OF 30

By Harold R. Mull and John C. Erickson, Jr.

Lewis Flight Propulsion Laboratory
Cleveland, Ohio

Washington
April 1957

NATIONAL ADVISORY COMMITTEE FOR AERONAUTICS

TECHNICAL NOTE 3978

SURVEY OF THE ACOUSTIC NEAR FIELD OF THREE NOZZLES AT A PRESSURE RATIO OF 30

By Harold R. Mull and John C. Erickson, Jr.

SUMMARY

Detailed measurements were made in the acoustic near field of three cold-air exhaust nozzles with pressure ratios of 30 exhausting into quiescent air. Two of the nozzles were convergent-divergent, one having a 15° conical expansion and the other an isentropic expansion. Throat diameters were 5/8 inch and exit diameters, 1.2 inches. The third nozzle was convergent with a 5/8-inch exit diameter.

The total acoustic power radiated by the jet stream was about the same for the convergent-divergent nozzles and appeared to be in agreement with predictions based upon tests at subsonic velocities and the Lighthill parameter. The convergent nozzle created more than the predicted noise power based on the Lighthill parameter. Contour maps and plots of the position of the maximum sound-pressure level for audible frequencies revealed that there were no intense sources of noise upstream of 10 nozzle-exit diameters from the jet exit. The 1/3-octave-band acoustic spectra showed a broad nonresonant shape. There were no discrete frequencies, and no high-level ultrasonic sources were detected.

INTRODUCTION

The use of rocket power for missiles and aircraft has focused attention on the noise fields created by the exhaust stream from high-pressure-ratio nozzles. The noise associated with high-velocity jets can be destructive to adjacent structures and cause failure of electronic equipment. Adequate knowledge of the intensity, spectrum, and directionality of the near-field noise is necessary to provide for the protection of delicate mechanisms and eliminate fatigue failure.

The near field, as the term implies, is that region which surrounds a distributed source out to a distance that is not long compared with an

acoustical wavelength. In the near field, the sound pressures are not in phase with the velocities; and the attenuation with distance of the sound pressures is, in general, greater than that from hemispherical expansion in the far field. For the higher frequencies, the measurement would include a portion of the far field.

From recent experimental studies (refs. 1-5), the near noise fields of subsonic and choked jets have been mapped in the horizontal plane through the jet axis. Further research, now under way, should improve the understanding of the mechanism of jet noise to the extent that the noise field can be predicted for standard nozzle configurations.

The complexities involved in operating a rocket motor make a small unheated air jet more suitable for near-noise-field studies. However, the results might be expected to apply to rockets if the difference in exit velocity is taken into account. Unpublished data covering small heated jets at temperatures up to 1000° F have shown no measurable effect of temperature on total sound power. For the rocket, the total sound power may be less than that predicted by the eighth-power curve of the velocity in the Lighthill parameter $\rho_0 A V^8 a_0^{-5}$ (ref. 6). The Lighthill parameter for the rocket exhaust stream would be near values associated with afterburning turbojets, and these were found to radiate less than the expected power (ref. 7) from extrapolation of an eighth-power curve resulting from measurements of a number of jets. One factor not included in the Lighthill parameter, the high pressure ratio, may also affect the noise power of the rocket.

In order to study the effect of nozzle design on the noise field, three designs were chosen. Two of the nozzles were convergent-divergent with fully expanded flow at a pressure ratio of 30, and a third was simply the convergent section of the first two. Figure 1 is a photograph of the three nozzles. One of the convergent-divergent nozzles had an isentropic (Laval) expansion and the other, a 15° conical expansion. The isentropic design provides the most uniform flow across the exit, and the 15° conical expansion is a common configuration used in rocket design. The 450-pound-per-square-inch plenum pressure is about that of the chamber pressure for some liquid-fuel rockets.

Although a pressure ratio of 30 would apply to a rocket only at sea level, this is also where the noise problem would be the most severe.

SYMBOLS

The following symbols are used in this report:

A area of jet exit, sq ft

a_0 speed of sound external to jet stream, ft/sec

d nozzle-exit diameter, ft

f frequency, cps

V jet-exit velocity, ft/sec

ρ_0 ambient density of medium outside of jet stream, slugs/cu ft

APPARATUS

Sectional drawings of the nozzles designed for this study of the near-field noise are shown in figure 2. The convergent section has an exit diameter of 0.625 inch. It was designed according to the method outlined in reference 8 in order to obtain a uniform exit speed. The two expansion units were bolted to the convergent unit to form the convergent-divergent nozzles. The isentropic expansion was designed by the method of reference 9. The jet-exit diameter of 1.206 inches allowed for fully expanded flow at a pressure ratio of 30. The 15° conical expansion was given the same jet-exit diameter as the isentropic nozzle.

The nozzles were mounted on a test stand located in the corner of a large room. A photograph of the test stand is shown in figure 3. The high-pressure air was supplied from a pressure- and temperature-regulated source through a remotely controlled 2-inch valve. From the valve the air traveled through a perforated-liner-type silencer to reduce the valve and pipe noise upstream of the nozzle. A short length of 8-inch pipe provided a plenum to which the convergent section was attached. Air pressure and temperature measurement stations were located in the plenum.

Sound-pressure measurements were made with a miniature condenser microphone. The microphone with its associated preamplifier was mounted on a stand so that the diaphragm of the microphone was at parallel incidence to the source (i.e., the diaphragm was in the horizontal plane through the jet axis). The power supply for the microphone was placed in a sound-proofed box at one side of the jet. The output was connected to a 1/3-octave-band analyzer with a spectrum recorder and a sound-level meter located in the control room adjacent to the test cell.

The measurement stations were located by means of lines ruled on a 4- by 8-foot sheet of plywood fastened to the floor. A schematic diagram of the test layout is shown in figure 4. Photographs of the airflow from the three nozzles were made by means of a single-pass schlieren system and camera.

A linear actuator coupled to an X-Y chart recorder was used to make total-head surveys. The total-head probe was mounted on a wedge, which was driven into the jet stream by the actuator. Movement of the chart was synchronized with the probe travel. A strain-gage pressure transducer was used to convert the total-head pressures to an electric signal.

PROCEDURE

Before beginning the sound-pressure-level survey of the near-field noise, the local velocity of the flow was determined by two methods. The conical shock formed by the impingement of the jet on a 20° cone placed in the jet stream near the jet exit was photographed by means of the schlieren system. The angle of shock was used to determine the Mach number for the expanded nozzles. Total-head surveys with an X-Y recorder were also used to survey the jet for the isentropic nozzle near the exit. The Mach number obtained from the preceding measurements agreed closely with the design Mach number for the isentropic nozzle.

Spectra were recorded at two positions in the reverberant field (i.e., outside the near field) before the start of the near-field survey. These spectra had nearly the same shape and amplitude for both positions. Typical spectra in the reverberant field are shown in figure 5. One of the stations in the reverberant field was about 15 feet from the nozzle and 35° from the jet axis; the other was about 20 feet from the nozzle and 135° from the jet axis.

The survey of the near-field noise was made by placing the microphone stand at one of the intersections of the grid and recording the spectra while the nozzle was operating. After the recording was made, the valve was closed and the microphone moved to a new position. This process was repeated going out from the 10° line until the reverberant level was reached at the lower frequencies. The over-all levels were monitored during the time the spectra were being recorded. Calibrations were made before and after each series of runs. The air-source pressure and temperature were closely regulated so that repeat runs gave identical results.

RESULTS AND DISCUSSION

Total Power

The total acoustic power[1] radiated by the jet during operation was computed from the reverberation level for each of the three nozzles.

[1]Acoustic terms in this report are used in accordance with the definitions given in reference 10.

The power radiated by the jet from the isentropic nozzle was 99 watts and from the conical nozzle, 78 watts. The jet from the convergent nozzle produced 26 watts of acoustic power.

A curve showing the relation of the Lighthill parameter $\rho_0 A V^8 a_0^{-5}$ to the total acoustic power of a number of jets of various sizes and velocities is included in reference 11. A total power of 90 watts for the convergent-divergent nozzles was predicted from this curve. This value is approximately midway between the measured power of the two convergent-divergent nozzles and about 1/2 decibel from both. The suggestion is made in reference 10 that Lighthill's parameter is correct for shock-free supersonic flow. Although the results reported in reference 10 are for a design Mach number of 1.36, the parameter still appears to be valid for other nozzles while operating at design conditions.

An effective velocity for the convergent nozzle was obtained from the computed thrust and mass flow. The use of this effective velocity in the Lighthill parameter predicted a power of 7.5 watts, which is well below the measured value of 26 watts. The computed thrust was 194 pounds for the convergent-divergent nozzles and 168 pounds for the convergent nozzle. Although, in a strict sense, the conical expansion is not isentropic, it is probably close enough to assume a thrust equal to that obtained with isentropic expansion.

The spectra in the reverberant field were similar for the convergent-divergent nozzles. These spectra can be compared with the power spectra resulting from tests of subsonic nozzles (ref. 7). The subsonic spectra indicate that a greater portion of the acoustic power is in the high frequencies and less in the low frequencies than with the supersonic spectra.

Spectra

Sample spectra for each of the three nozzles are presented in figure 6 for a single point. The point selected was 2 feet downstream and on the 10° line from the jet exit. This would be 20 nozzle-exit diameters downstream for the convergent-divergent nozzles and 38 nozzle-exit diameters downstream for the convergent nozzle. The values have been adjusted to equivalent spectrum levels by reducing the measured sound-pressure level to that within a band 1 cycle wide centered at the frequency plotted on the graph. The spectra are all essentially flat up to about 3000 cycles per second, from which they decay at about 6 to 12 decibels per octave. Moderate differences were noted in spectra at other points, but the broad nonresonant shape of the spectra persisted. This is in direct contrast with jets from convergent nozzles being

operated just above choking, where the stationary shock pattern produces a definite pitch which stands out over the rest of the jet noise (ref. 4).

Over-all Sound-Pressure-Level Curves

The over-all sound-pressure-level curves are presented in figure 7. In figure 7(a) the dashed portion of the curve represents the estimated free-field levels obtained by substracting the reverberant level from the measured value. Since the uncorrected curves are close together, the single curve corrects both measured curves. Where the difference is greater than 10 decibels, corrections are less than 1 decibel.

These curves (fig. 7(a)) clearly show that the predominant sources of noise are between 20 and 35 nozzle-exit diameters downstream of the nozzle exit. The shapes of the curves for the isentropic and conical nozzles are very similar. The absence of a sharp peak shows that there is a wide distribution of noise sources along the jet boundary. A corresponding curve for a jet engine from reference 1 is plotted in figure 7 for comparison. The general shape of the curve from the convergent jet (fig. 7(b)) is more like that of the jet engine.

The over-all sound-pressure-level curves in figure 7(a) rise 3 to 5 decibels in the region from 5 to 10 nozzle-exit diameters (6 in.). The level of the curve in this region suggests that sound-pressure levels near the jet exit would be lower in the field, where there would be no masking effect of the reverberant sound in a room. The curves in figure 7(a) reach a maximum near 30 nozzle-exit diameters downstream and then gradually fall 11 decibels below the maximum at 75 nozzle-exit diameters.

Contour maps showing lines of equal sound-pressure level are shown for each of the three nozzles in figures 8 to 10. These figures include over-all curves as well as the 1/3-octave bands with center frequencies of 100, 315, 1000, 3150, and 10,000 cycles per second. In order to allow easier comparison with the other types of band analyzers, the 1/3-octave-band levels have been reduced to corresponding spectrum levels. In addition, all the curves have been corrected for reverberant sound. The numbers on the lines indicate the sound-pressure level contributed by a band 1 cycle wide centered at the stated frequency in the free field.

The contour maps of the jet noise from the isentropic nozzle are shown in figure 8. The over-all curve shows the principal acoustic sources to be about 27 nozzle-exit diameters downstream of the jet exit. This correlates with the contours for the frequency bands since they indicate the same area of noise source. The exception is the 10,000-cycle contour in which the noise source appears to be about 15 nozzle-exit diameters downstream. However, the level of the 10,000-cycle band is much lower than that of the lower frequencies.

The angle of propagation for the over-all noise can be determined by drawing a line through the farthest point from the jet axis on each of the equal-pressure lines. This line was found to lie at an angle of 51° with the jet axis and to cross the jet axis at a point 27 nozzle-exit diameters downstream. This could result in an angle approaching 45° for far-field contours with the jet exit taken as the center of the source.

The low-frequency contours exhibit a double-peaked structure. This is possibly caused by two physically separated sources of sound at that frequency. This "second source" is also noted in reference 1 for frequencies below 100 cycles per second.

The sound-pressure-level contours for the conical nozzle are presented in figure 9. The angle of propagation of the noise from the jet stream of the conical nozzle is about 39°. The outer contour line shows a tendency to curve away from the 39° line. Probably the angle of maximum propagation would again be nearly 45° in the far field. A line through the highest points of the contours would cross the jet axis at 26 nozzle-exit diameters downstream.

The contours for the noise from the convergent nozzle are shown in figure 10. Here the angle of propagation with the jet axis is about 13°, and the intersection with the jet axis of a line through the maximum points of the contours is 5 nozzle-exit diameters downstream. The elongated pattern is quite different from that of the other two nozzles. This is probably due to the presence of a series of strong shocks downstream of the jet exit.

Noise Source

Figure 11 is a plot of the apparent source position of the noise in each of the 1/3-octave bands. The points in figure 11 were obtained for the convergent-divergent nozzles by plotting the location of the maximum sound-pressure level for each 1/3-octave band along the 10° line. Because of the many strong standing shocks, the noise-source positions for the convergent nozzle are too scattered to plot. The dimensionless frequency or Strouhal number $f\frac{d}{V}$ and the distance downstream of the jet exit in nozzle-exit diameters were used as the parameters to allow direct comparison with other jets. Figure 11 also includes similar data (ref. 1) from the near noise field of the exhaust stream of a jet engine.

From the curves of figure 11 it is apparent that the noise sources are several nozzle-exit diameters downstream of those resulting from subsonic jet turbulence (ref. 1). There are no strong sources upstream of 10 nozzle-exit diameters. The cluster of noise sources around the

25- to 30-diameter position partially explains the larger over-all level measured in that region. The lower-frequency end of the curve corresponds to the extrapolated end of the subsonic curve, indicating that the noise-source positions are again the same for the dimensionless case when the jet reached a subsonic speed.

Studies of the characteristics (ref. 12) of five supersonic jets exhausting into free air have shown that, after the jet decays to sonic velocity, it can be treated as a simple parallel-flow jet. The sonic point was at about 30 nozzle-exit diameters for a Mach 2.87 jet (ref. 11). There was very little spreading upstream of 10 nozzle-exit diameters, and the Mach 3 jets did not expand to a double-exit diameter until 20 nozzle-exit diameters downstream.

It should be emphasized that figure 11 is a plot showing the position of the maximum pressure level for each 1/3-octave band and not the frequency of the spectral peaks along the boundary. Although a frequency may have the highest pressure level in a certain spectrum, its level may be greater at another location.

Schlieren Photographs

Schlieren photographs of the flow patterns immediately downstream of the nozzle exit of each of the three nozzles are shown in figure 12. The smooth parallel flow interlaced with Mach lines from the isentropic nozzle is in sharp contrast with the strong shocks from the other two nozzles. The pattern for the convergent nozzle is the well-known shock diamond, which is repeated several times downstream of the field of view of the schlieren apparatus. Although the exit diameter of the convergent nozzle is only a little over half that of the other two nozzles, the flow near the exit has already expanded to a larger diameter than the flow from the convergent-divergent nozzles. This explosive bursting of the stream is typical of the strongly overchoked convergent nozzle. Turbulence is evident along the edges of all three patterns.

Ultrasonic Noise

Although ultrasonic noise was not surveyed during this investigation, some effort was made to detect the presence of ultrasonic frequencies in the spectra near the jet exit. Two attempts were made to measure the ultrasonic frequencies out to 50,000 cycles per second by extending the frequency range of the analysis with an ultrasonic spectrum analyzer. With both the condenser microphone and a very small crystal microphone, the apparent ultrasonic level was very much lower than the levels of the audible noise described. There were no sharp peaks in the ultrasonic spectrum. This result was not unexpected, since any shock system at these pressure values would be widely spaced and would radiate at lower frequencies (ref. 4).

SUMMARY OF RESULTS

Measurements made in the near acoustic noise field of three exhaust nozzles with pressure ratios of 30 showed that:

1. The total acoustic power radiated by the jet stream from two convergent-divergent nozzles was nearly the same, that is, 99 watts for the isentropic nozzle and 78 watts for the conical nozzle.

2. The total acoustic power radiated by the two convergent-divergent nozzles was about that predicted from tests of subsonic jets and the Lighthill parameter (90 w).

3. The convergent nozzle generated much more noise than predicted from the Lighthill parameter; the measured noise was 26 watts and the predicted noise, 7.5 watts.

4. The power spectra (reverberant field) were similar for the convergent-divergent nozzles; the corresponding spectra for subsonic nozzles indicated more high-frequency and less low-frequency power.

5. Spectra taken at a distance of 2 feet downstream of the exit and at an angle of 10° from the jet axis were essentially flat to 3000 cycles per second and decayed at about 6 to 12 decibels per octave above 3000 cycles per second. Spectra recorded at other points were similar in shape. No sharp peaks were seen in any of the recorded spectra.

6. For the convergent-divergent nozzles, over-all sound-pressure-level curves along the 10° line from the jet exit reached their peak level at about 30 nozzle-exit diameters downstream and fell slowly downstream. Levels near the jet exit were much lower than the maximum.

7. Contour maps of the near-field noise revealed that:

   (a) For the isentropic nozzle, the over-all noise was radiated from an apparent source 27 nozzle-exit diameters downstream of the jet exit at an angle of 51° from the axis.

   (b) For the conical nozzle, the angle of maximum propagation for the jet noise was 39° and the apparent noise source was 26 nozzle-exit diameters downstream.

   (c) For the convergent nozzle, corresponding values of angle of propagation and location of noise source were 13° and 5 nozzle-exit diameters, respectively.

8. The methods used to locate the position of the noise sources in the 1/3-octave band revealed that there were no strong noise sources upstream of 10 nozzle-exit diameters for both the isentropic and the conical nozzles.

9. No strong sources of ultrasonic noise were found.

Lewis Flight Propulsion Laboratory
National Advisory Committee for Aeronautics
Cleveland, Ohio, February 7, 1957

REFERENCES

1. Howes, Walton L., and Mull, Harold R.: Near Noise Field of a Jet-Engine Exhaust. I - Sound Pressures. NACA TN 3763, 1956.

2. Callaghan, Edmund E., Howes, Walton L., and Coles, Willard D.: Near Noise Field of a Jet-Engine Exhaust. II - Cross Correlation of Sound Pressures. NACA TN 3764, 1956.

3. Westley, R., and Lilley, G. M.: An Investigation of the Noise Field from a Small Jet and Method for Its Reduction. Rep. No. 53, The College Aero. (Cranfield), Jan. 1952.

4. Lassiter, Leslie W., and Heitkotter, Robert H.: Some Measurements of Noise from Three Solid-Fuel Rocket Engines. NACA TN 3316, 1954.

5. Powell, A.: On the Mechanism of Choked Jet Noise. Proc. Phys. Soc., sec. B, pt. 12, vol. 66, no. 408B, Dec. 1953, pp. 1039-1056.

6. Lighthill, J. M.: On Sound Generated Aerodynamically. I - General Theory. Proc. Roy. Soc. (London), ser. A, vol. 211, no. 1107, Mar. 20, 1952, pp. 564-587.

7. Coles, Willard D., and Callaghan, Edmund E.: Investigation of the Far Noise Field of Jets. II - Comparison of Air Jets and Jet Engines. NACA TN 3591, 1956.

8. Smith, Richard H., and Wang, Chi-Teh: Contracting Cones Giving Uniform Throat Speeds. Jour. Aero. Sci., vol. 11, no. 4, Oct. 1944, pp. 356-361.

9. Foelsch, Kuno: The Analytical Design of an Axially Symmetric Laval Nozzle for a Parallel and Uniform Jet. Jour. Aero. Sci., vol. 16, no. 3, Mar. 1949, pp. 161-167.

10. Bolt, R. H., Lukasik, S. J., Nolle, A. W., and Frost, A. D., eds.: Handbook of Acoustic Noise Control. Vol. 1. Physical Acoustics. WADC Tech. Rep. 52-204, Aero. Medical Lab., Wright Air Dev. Center, Wright-Patterson Air Force Base, Dec. 1952. (Contract No. AF 33(038)-20572, RDO No. 695-63.)

11. Callaghan, Edmund E., Sanders, Newell D., and North, Warren J.: Recent NACA Investigations of Noise-Reduction Devices for Full-Scale Engines. Aero. Eng. Rev., vol. 14, no. 6, June 1955, p. 66.

12. Anderson, Arthur R., and Johns, Frank R.: Characteristics of Free Supersonic Jets Exhausting into Quiescent Air. Jet Prop., vol. 25, no. 1, Jan. 19, 1955, pp. 13-15.

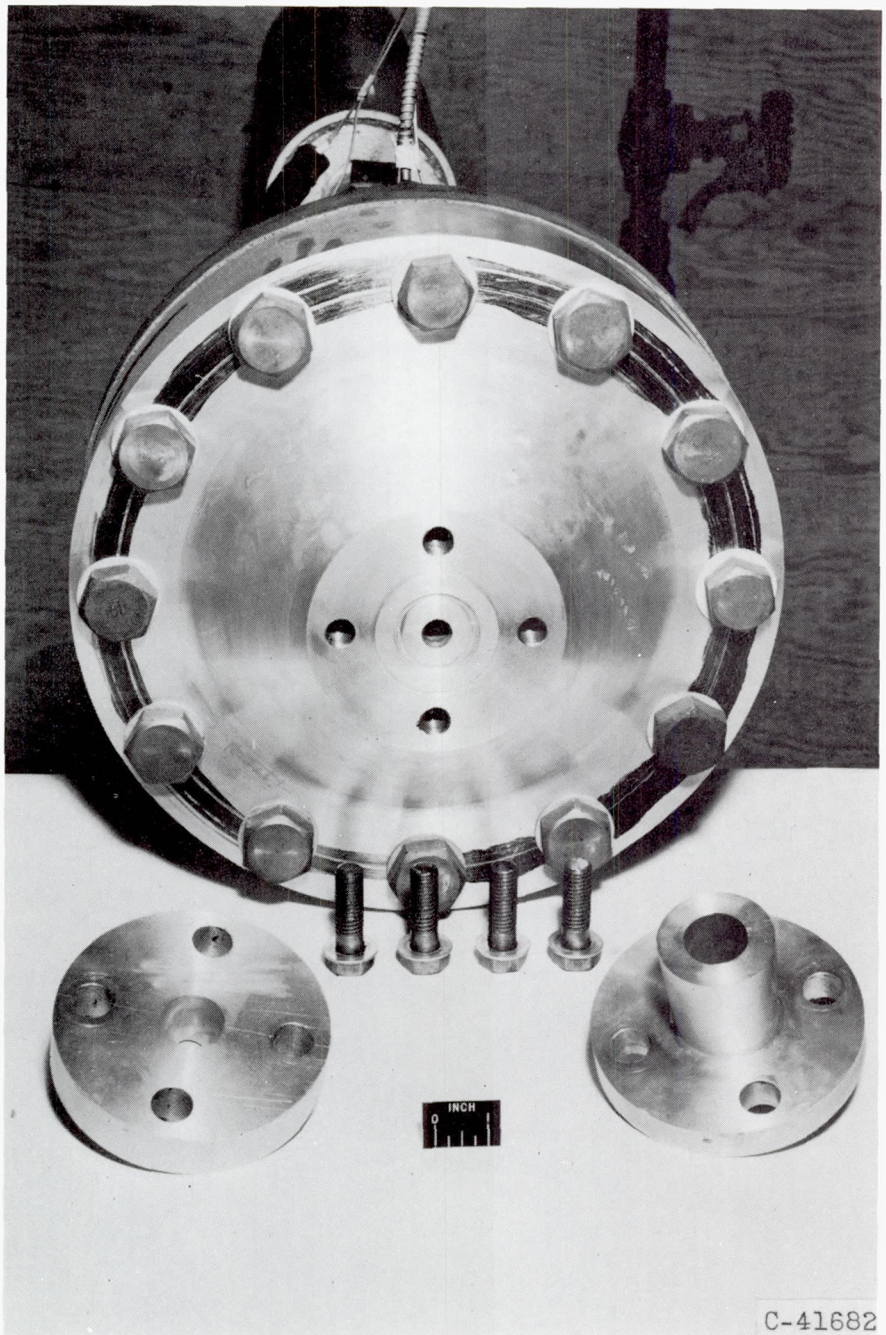

Figure 1. - Upstream view of nozzle test rig with convergent nozzle attached, 15° conical nozzle (on left), and isentropic nozzle (on right).

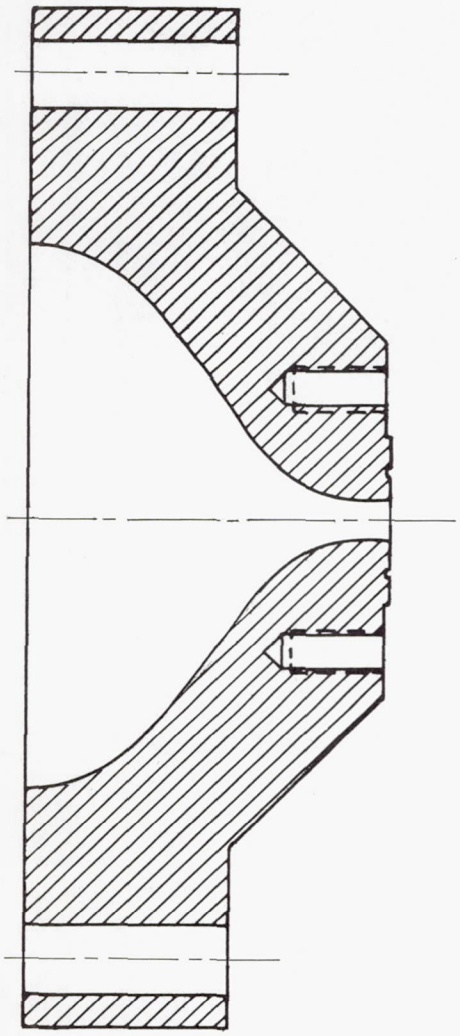

(a) Convergent nozzle; jet-exit diameter 0.625 inch.

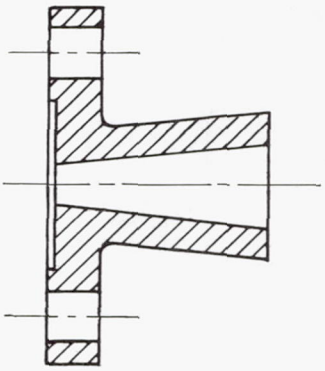

(b) Isentropic nozzle; jet-exit diameter, 1.206 inches; throat diameter, 0.625 inch.

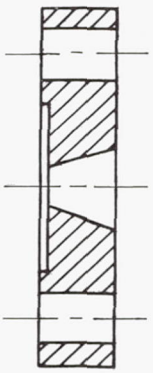

(c) Conical nozzle; jet-exit diameter, 1.206 inches; throat diameter, 0.625 inch.

Figure 2. - Test nozzles.

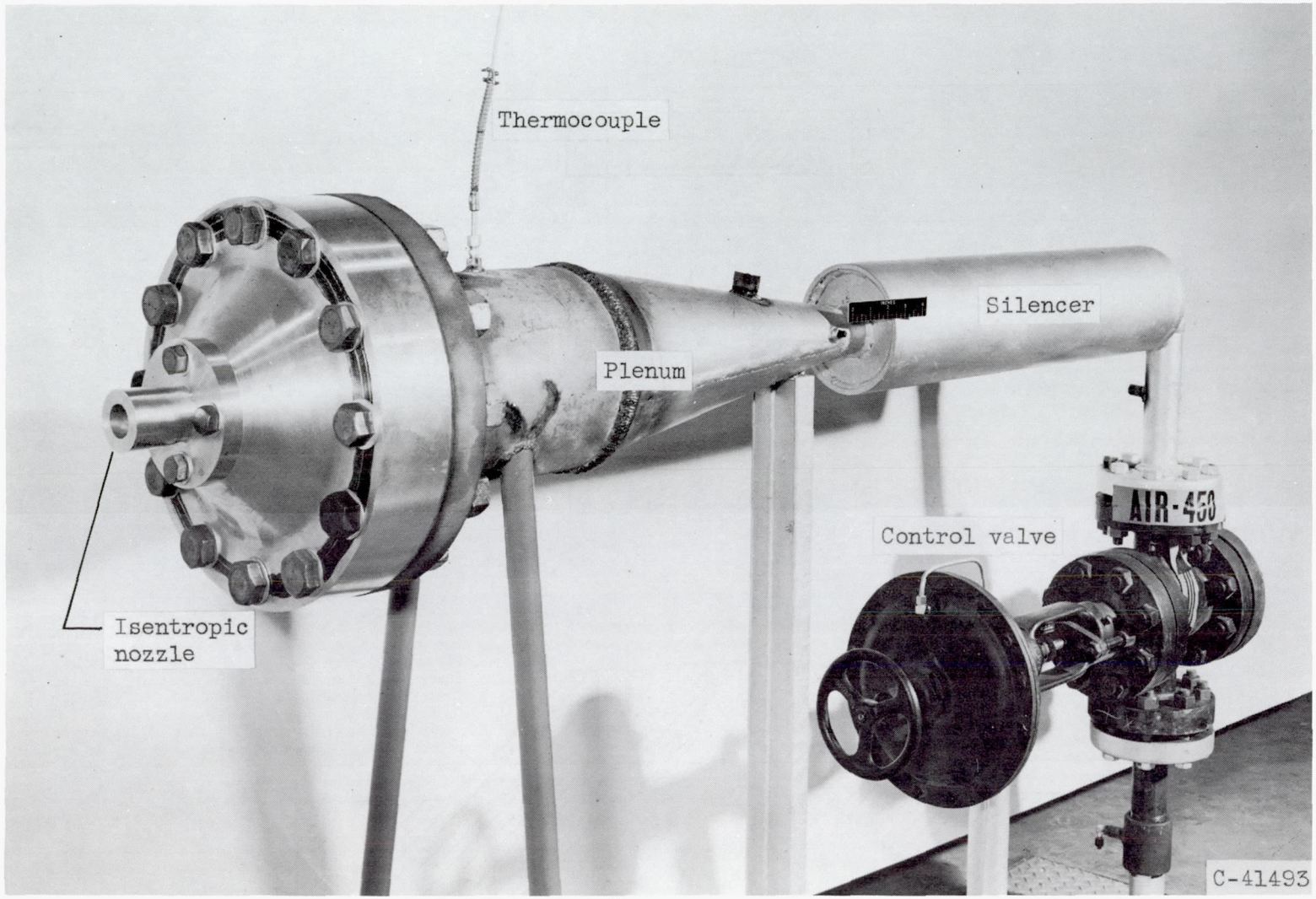

Figure 3. - Side view of test rig with isentropic nozzle attached to convergent section.

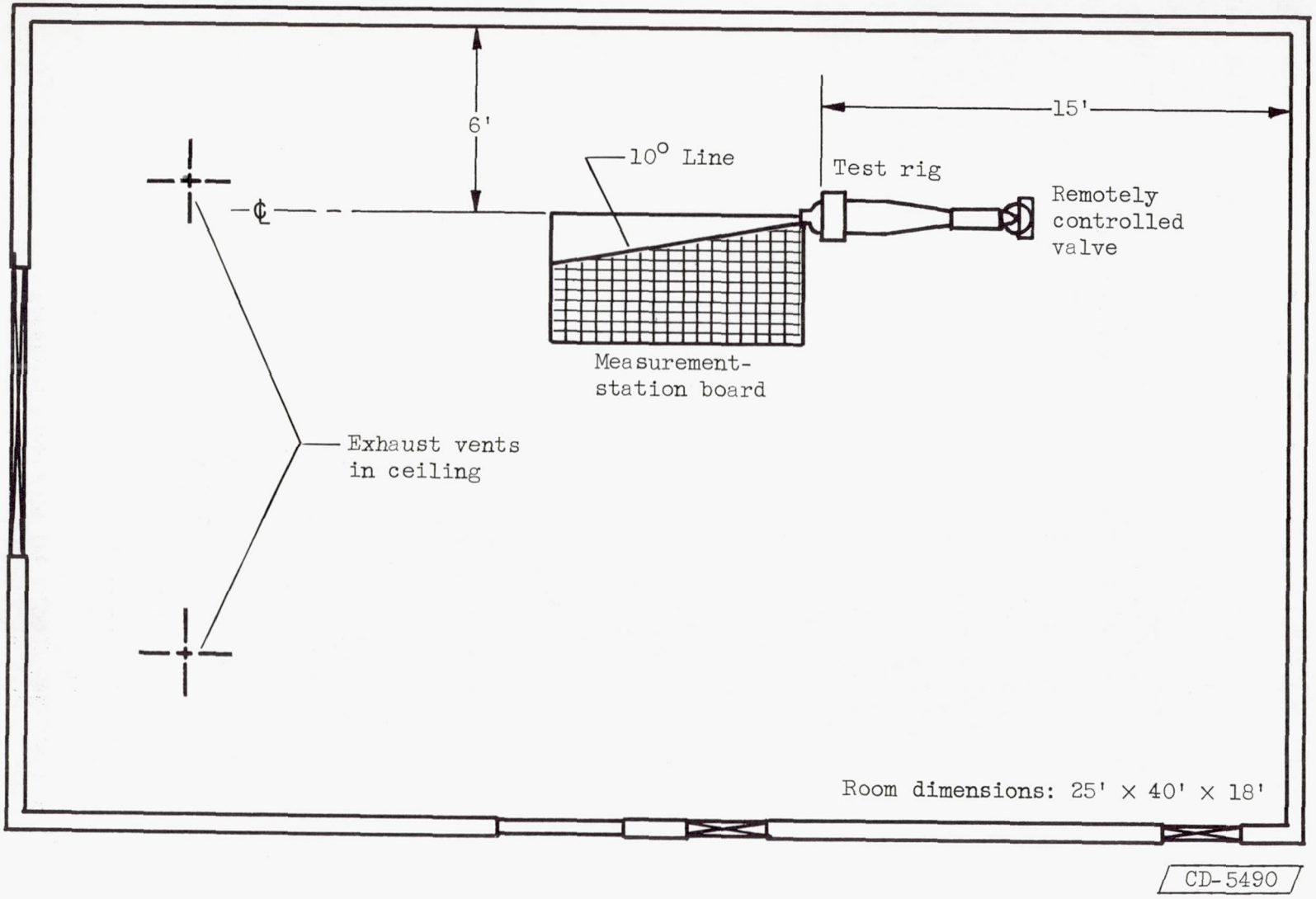

Figure 4. - Schematic diagram of test cell and measurement stations.

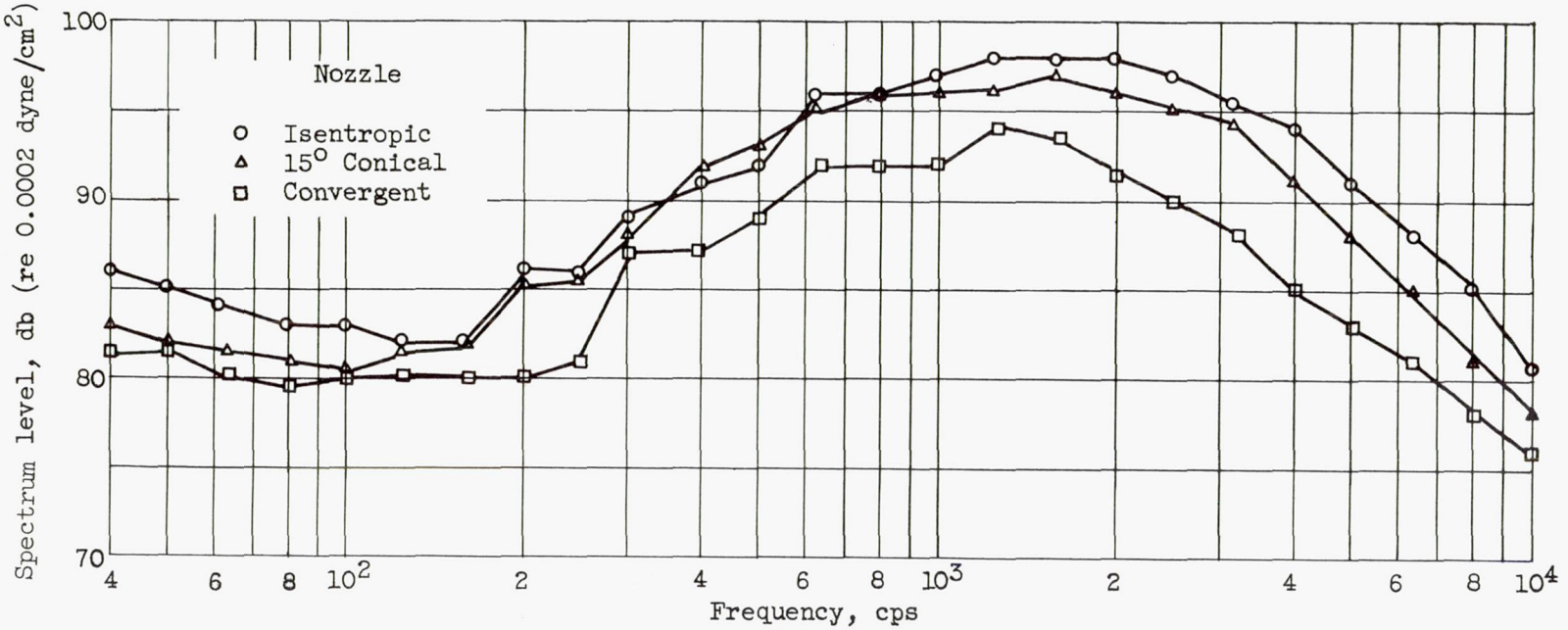

Figure 5. - Acoustic spectra in reverberant field.

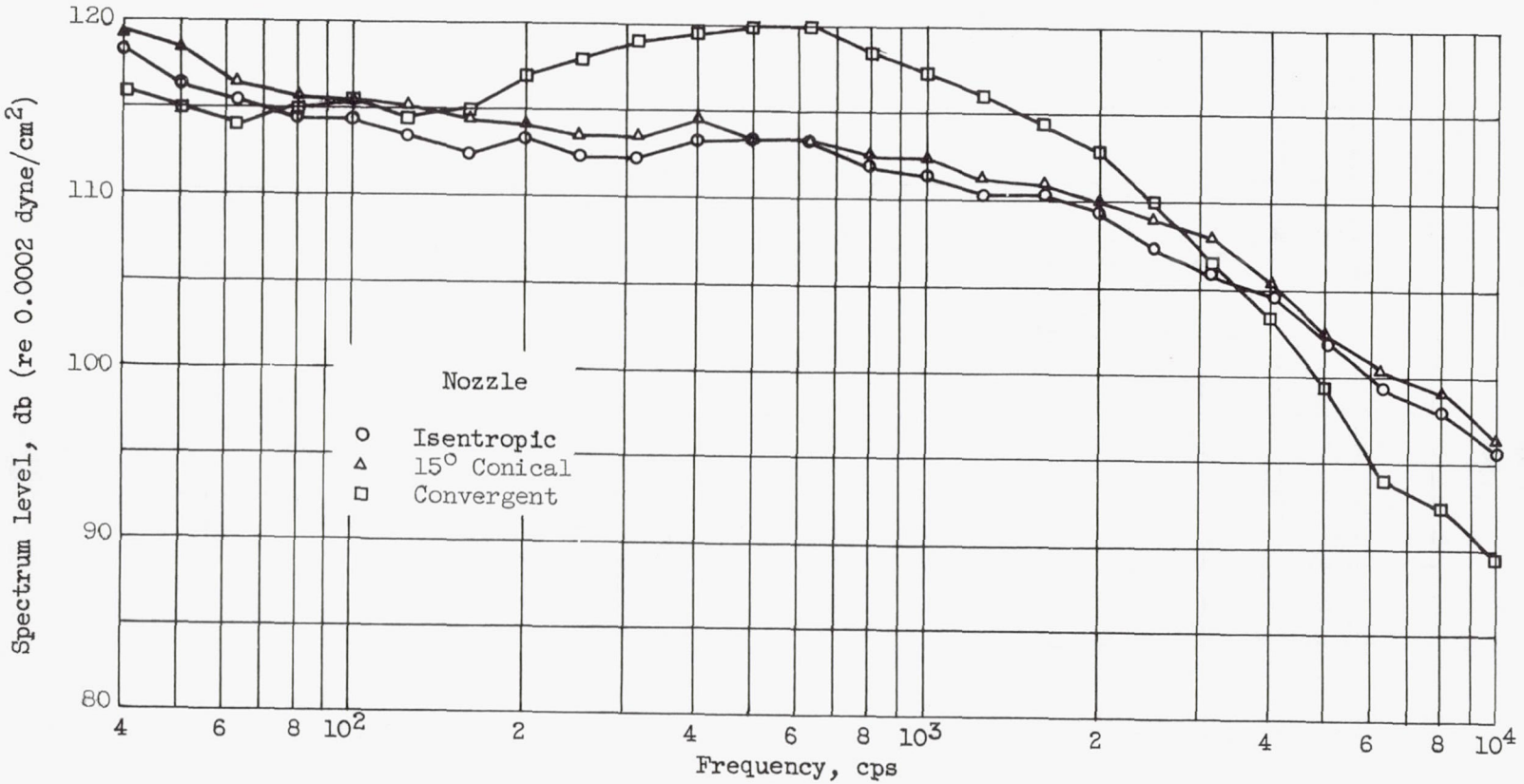

Figure 6. - Noise spectra 2 feet from jet exit on 10° line.

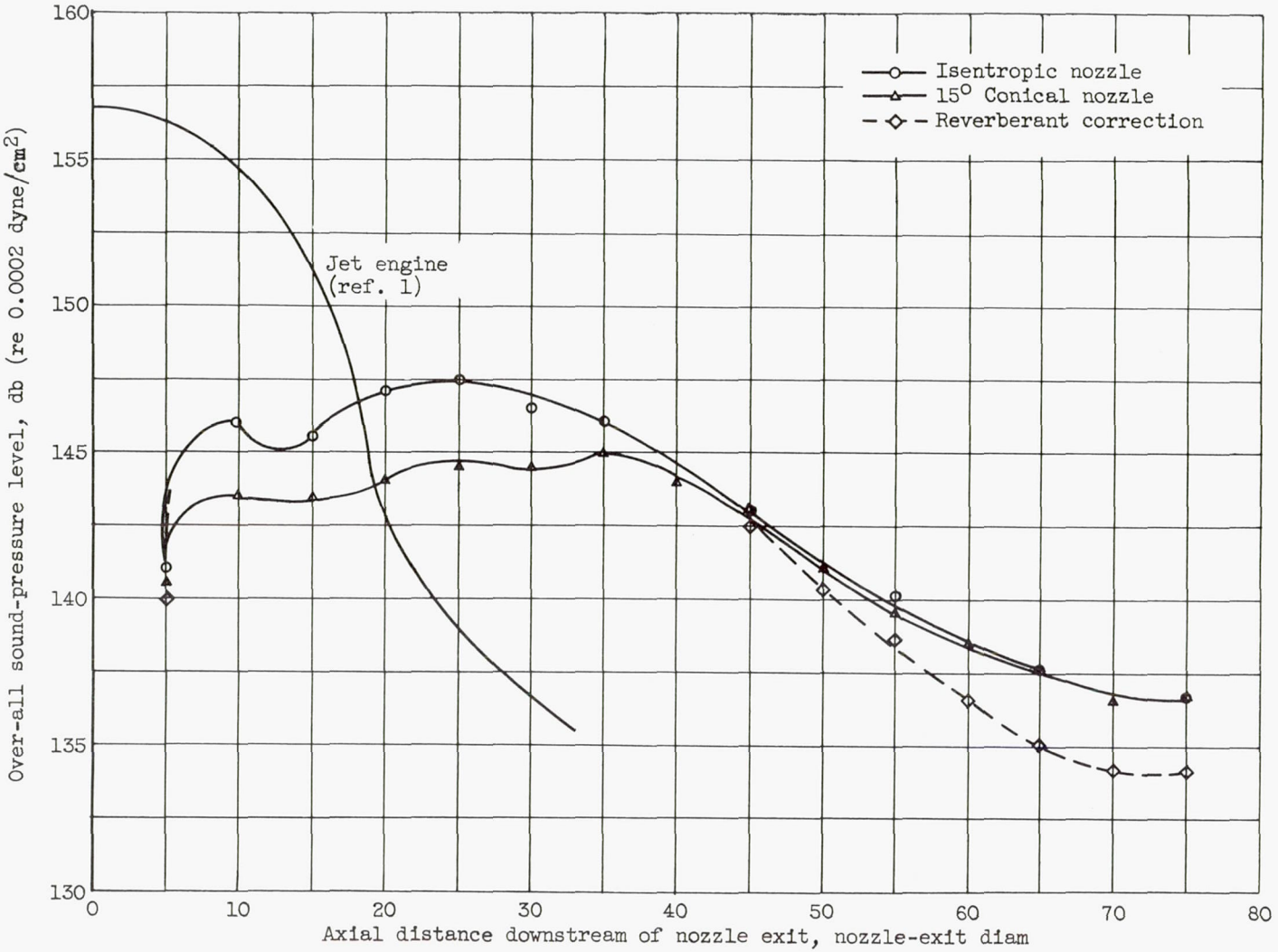

(a) Convergent-divergent nozzles.

Figure 7. - Over-all sound pressure along 10° line from jet exit.

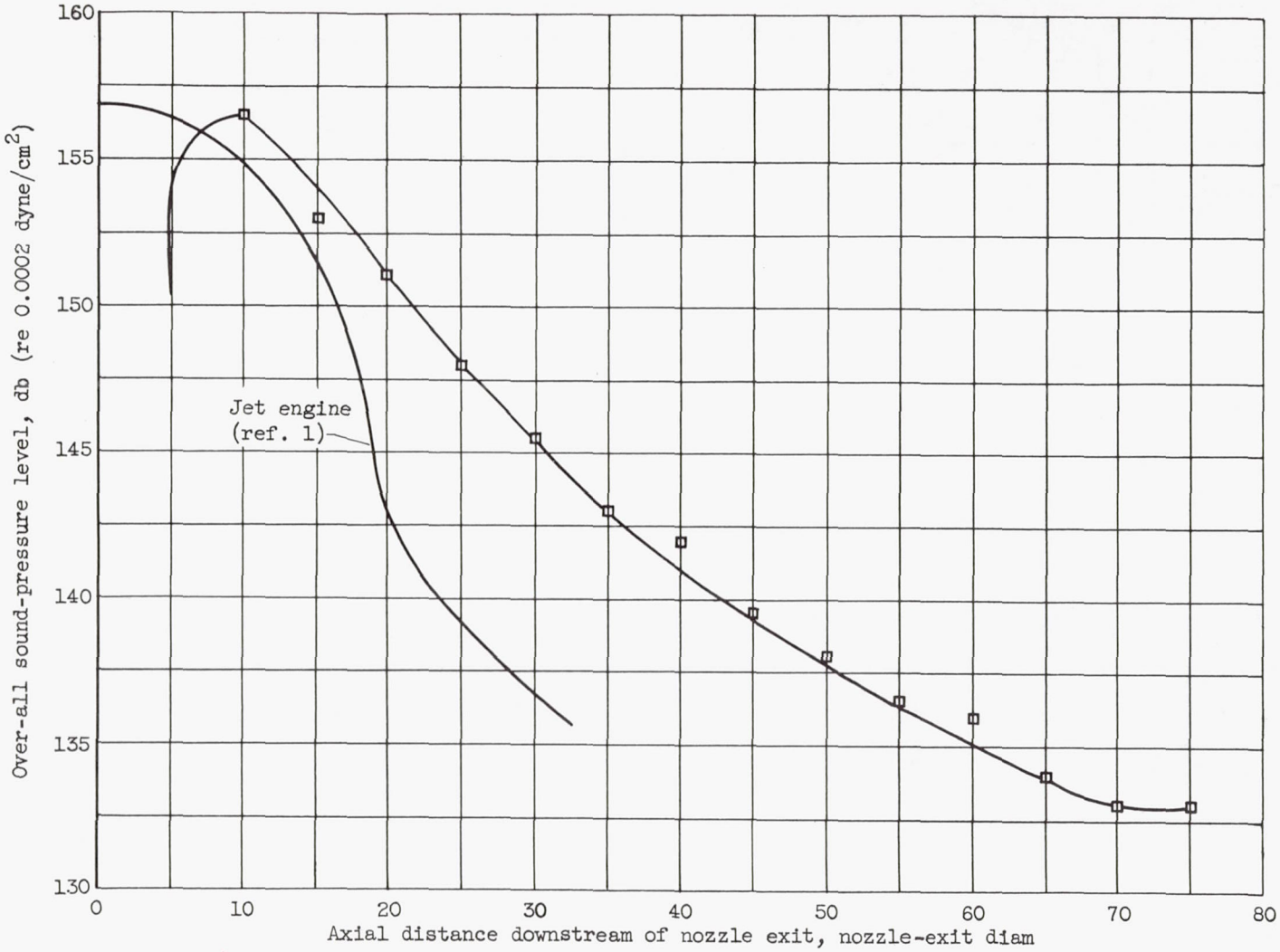

(b) Convergent nozzle.

Figure 7. - Concluded. Over-all sound pressure along 10° line from jet exit.

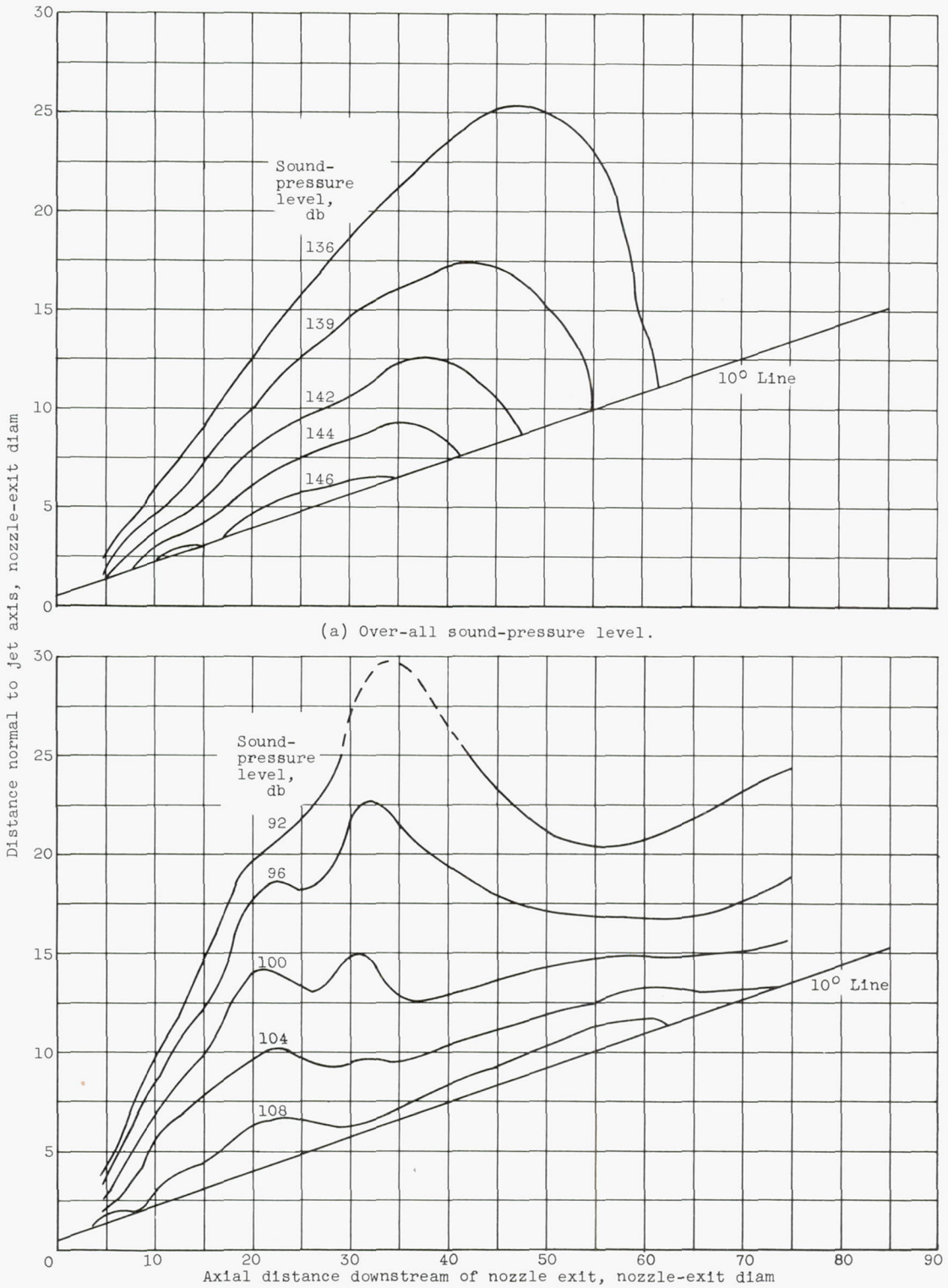

(a) Over-all sound-pressure level.

(b) Frequency band, 89 to 112 cycles per second.

Figure 8. - Near-field contours of noise from isentropic nozzle.

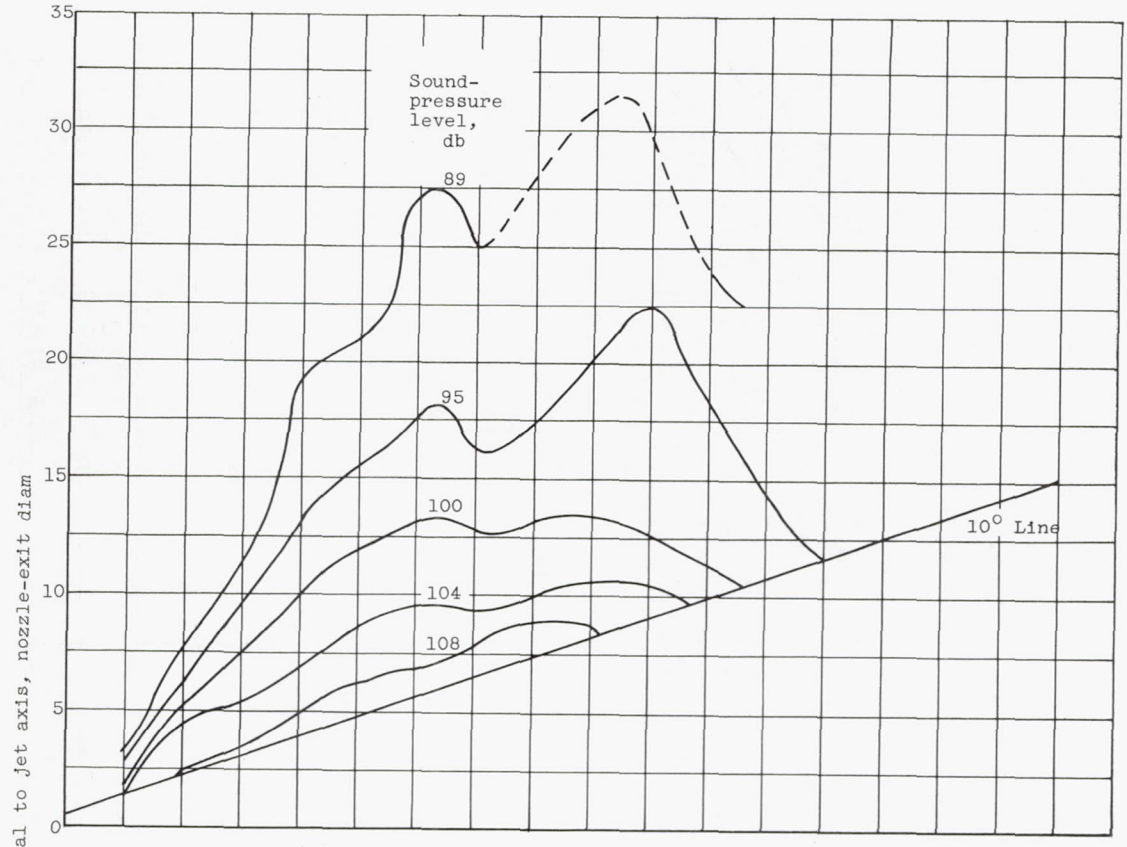

(c) Frequency band, 282 to 355 cycles per second.

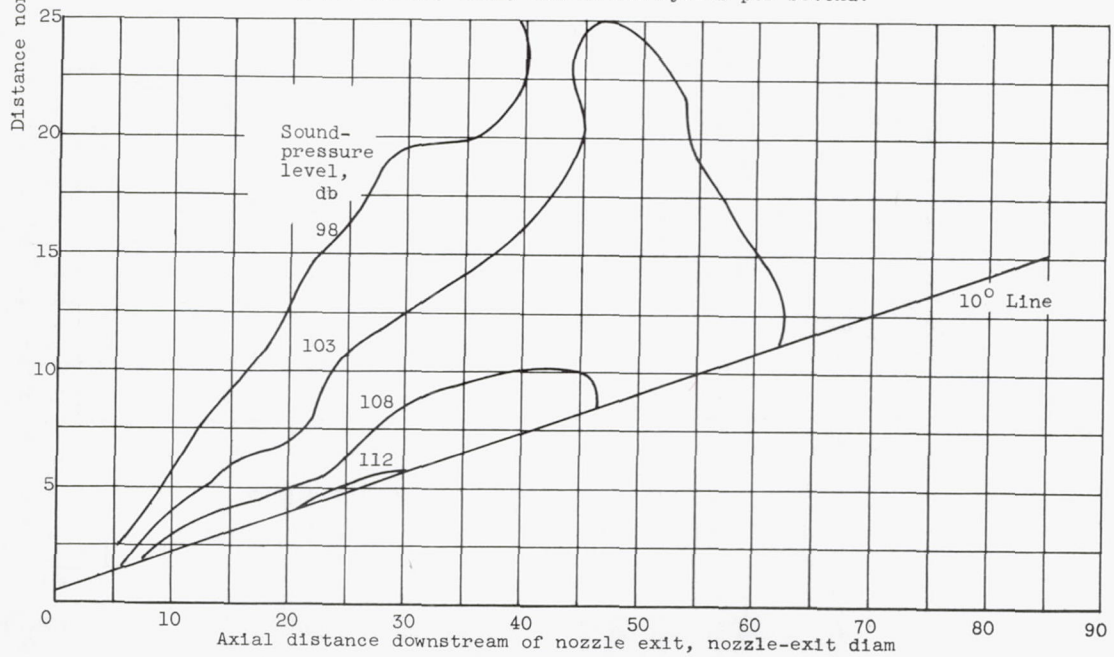

(d) Frequency band, 891 to 1120 cycles per second.

Figure 8. - Continued. Near-field contours of noise from isentropic nozzle.

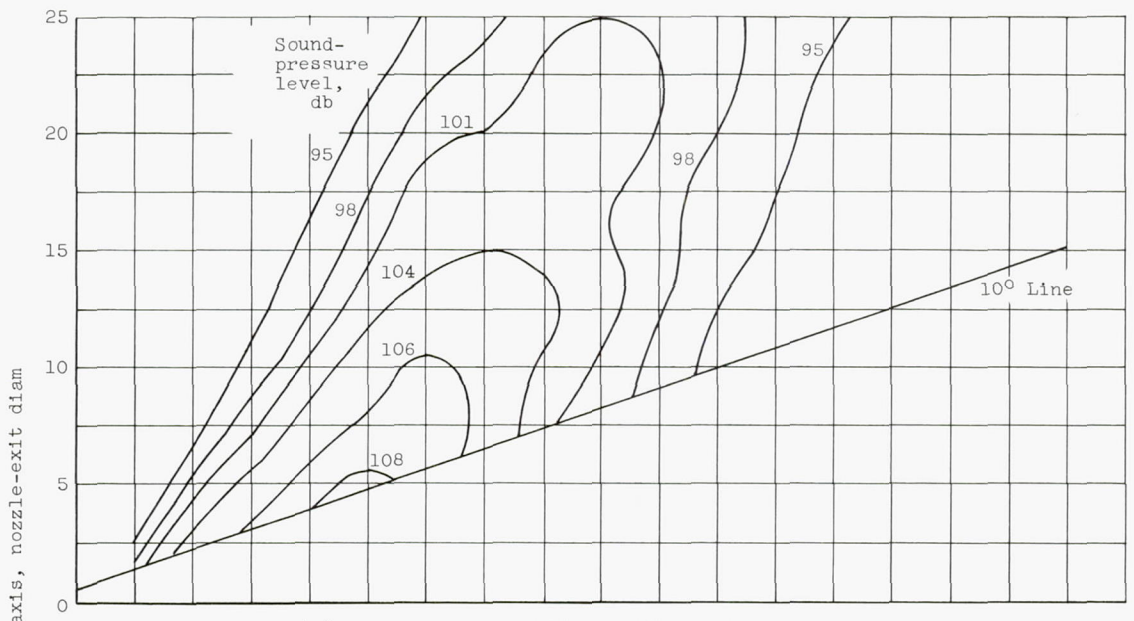

(e) Frequency band, 2820 to 3550 cycles per second.

(f) Frequency band, 8910 to 11,200 cycles per second.

Figure 8. - Concluded. Near-field contours of noise from isentropic nozzle.

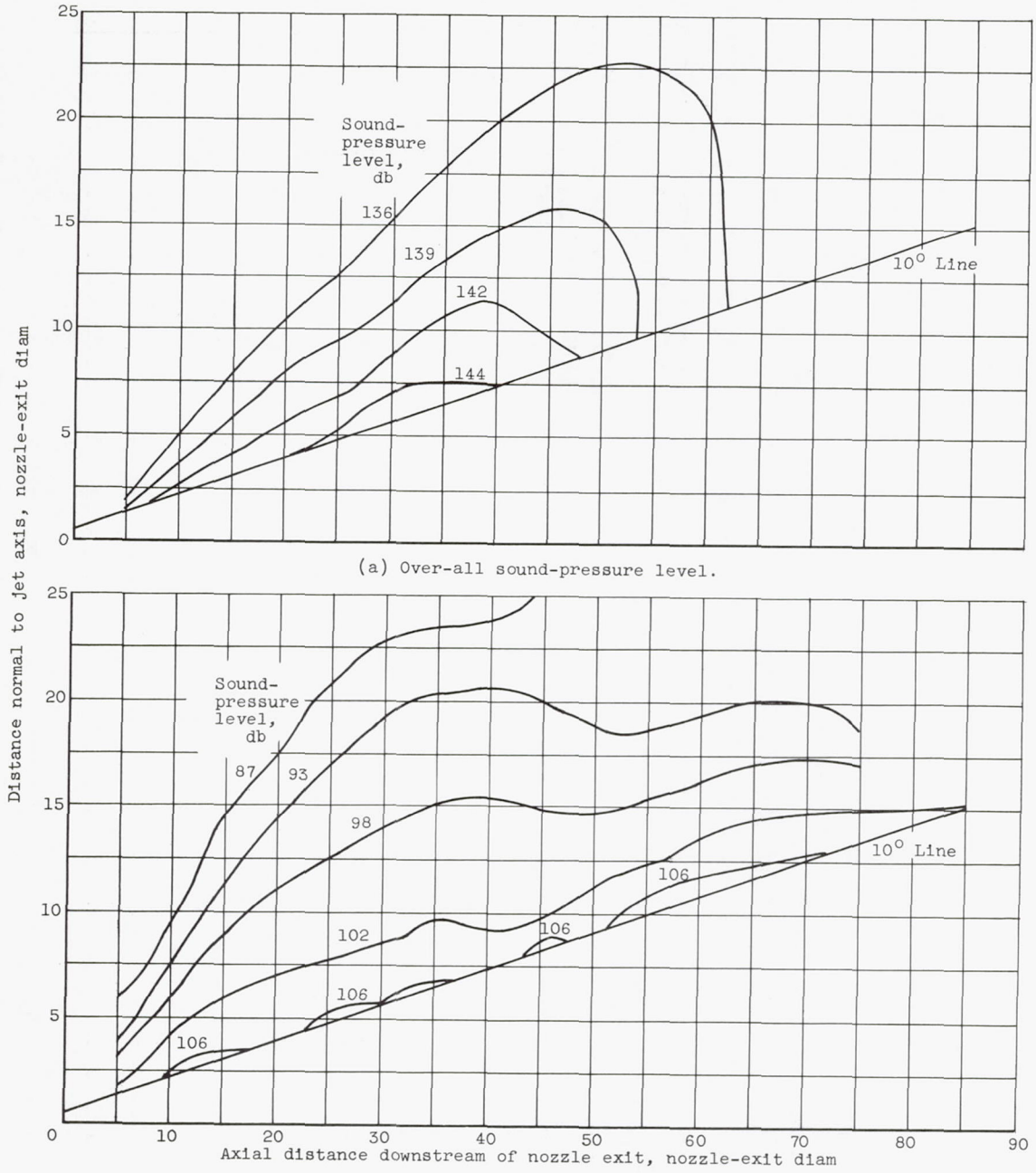

(a) Over-all sound-pressure level.

(b) Frequency band, 89 to 112 cycles per second.

Figure 9. - Near-field contours of noise from 15° conical nozzle.

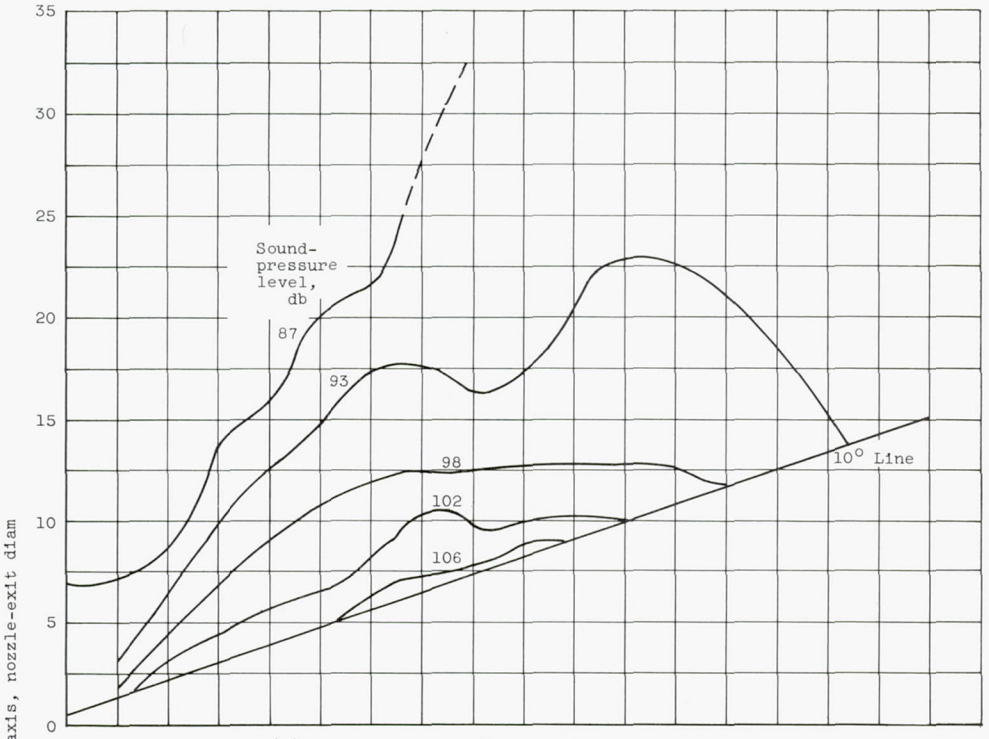

(c) Frequency band, 282 to 355 cycles per second.

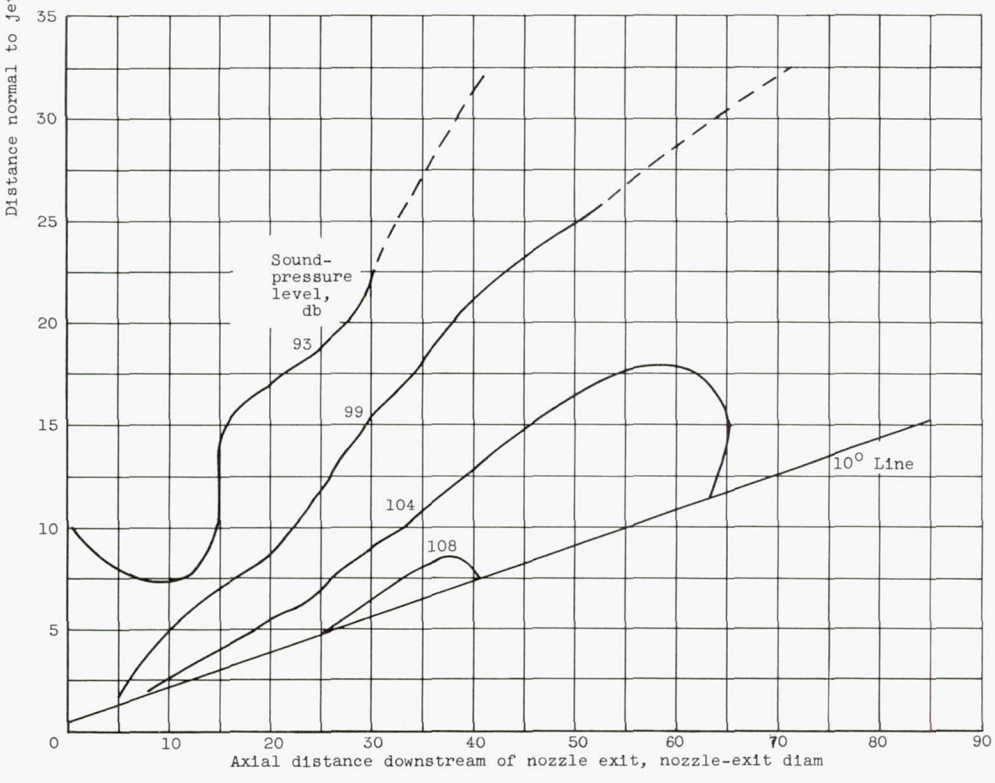

(d) Frequency band, 891 to 1120 cycles per second.

Figure 9. - Continued. Near-field contours of noise from 15° conical nozzle.

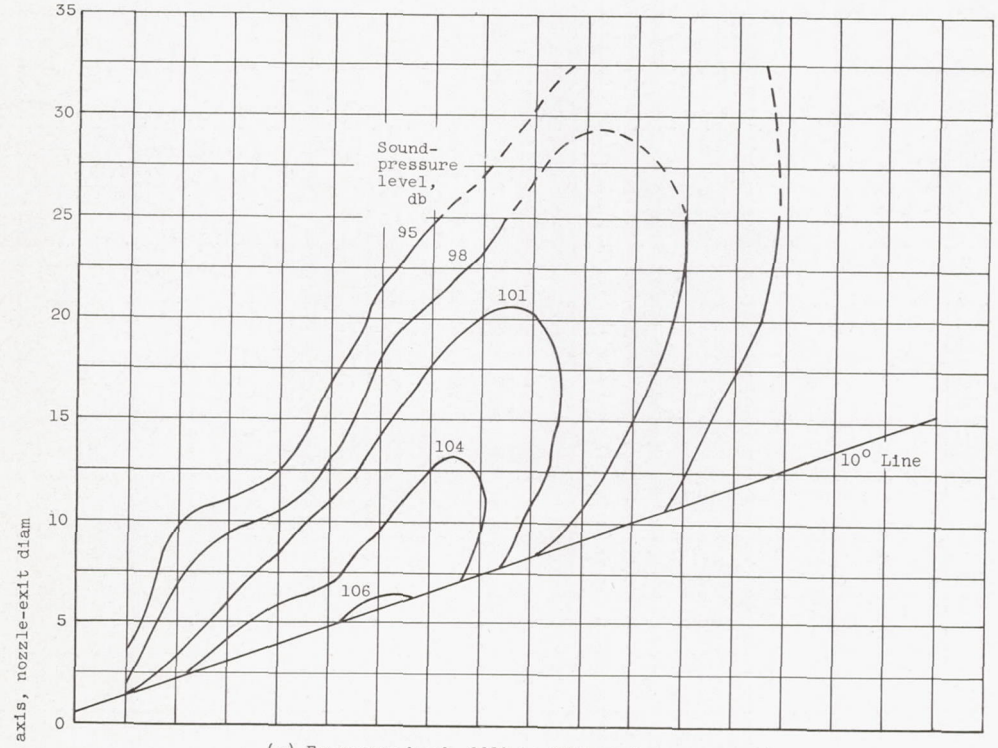

(e) Frequency band, 2820 to 3550 cycles per second.

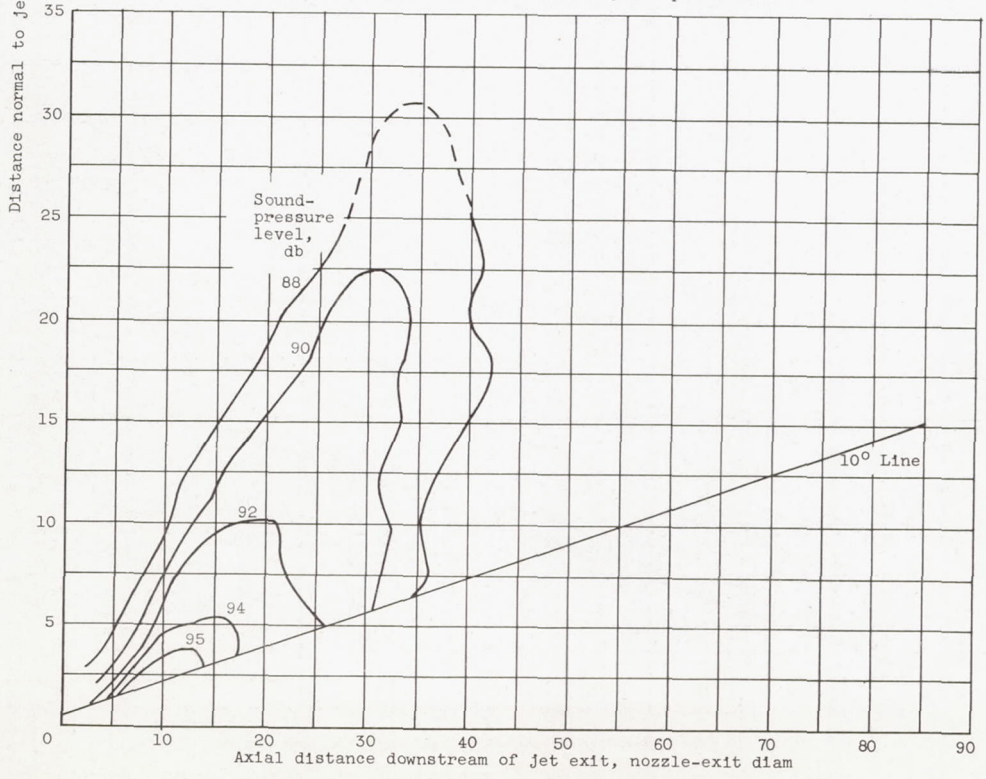

(f) Frequency band, 8910 to 11,200 cycles per second.

Figure 9. - Concluded. Near-field contours of noise from 15° conical nozzle.

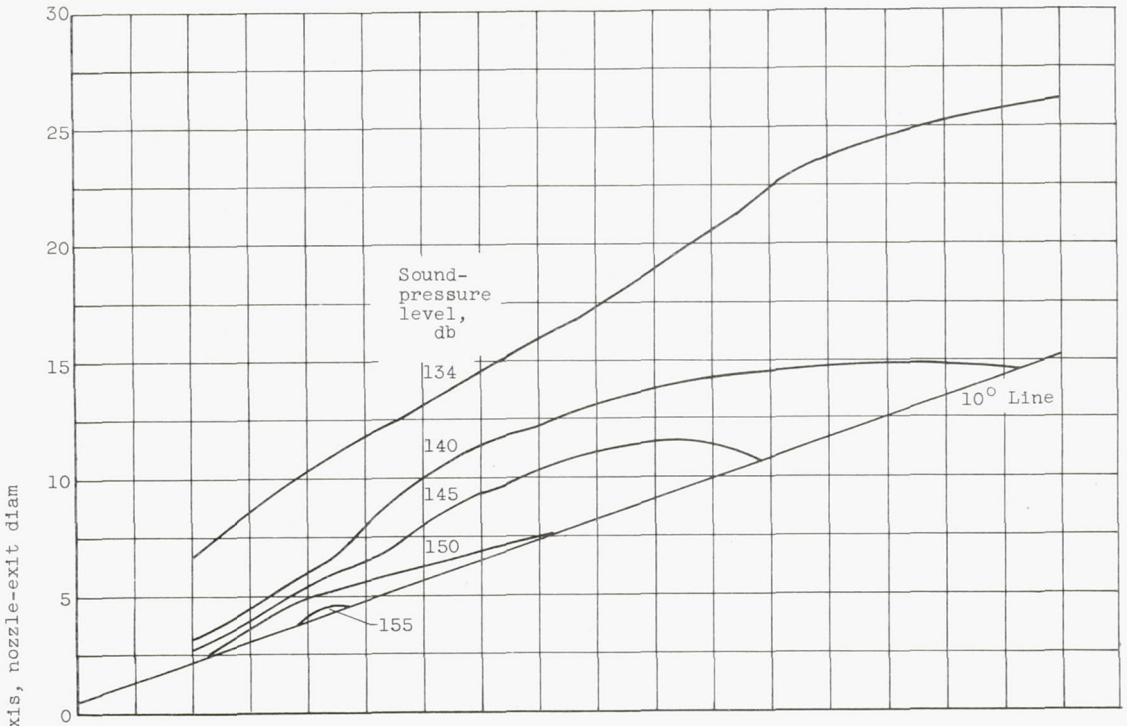

(a) Over-all sound-pressure level.

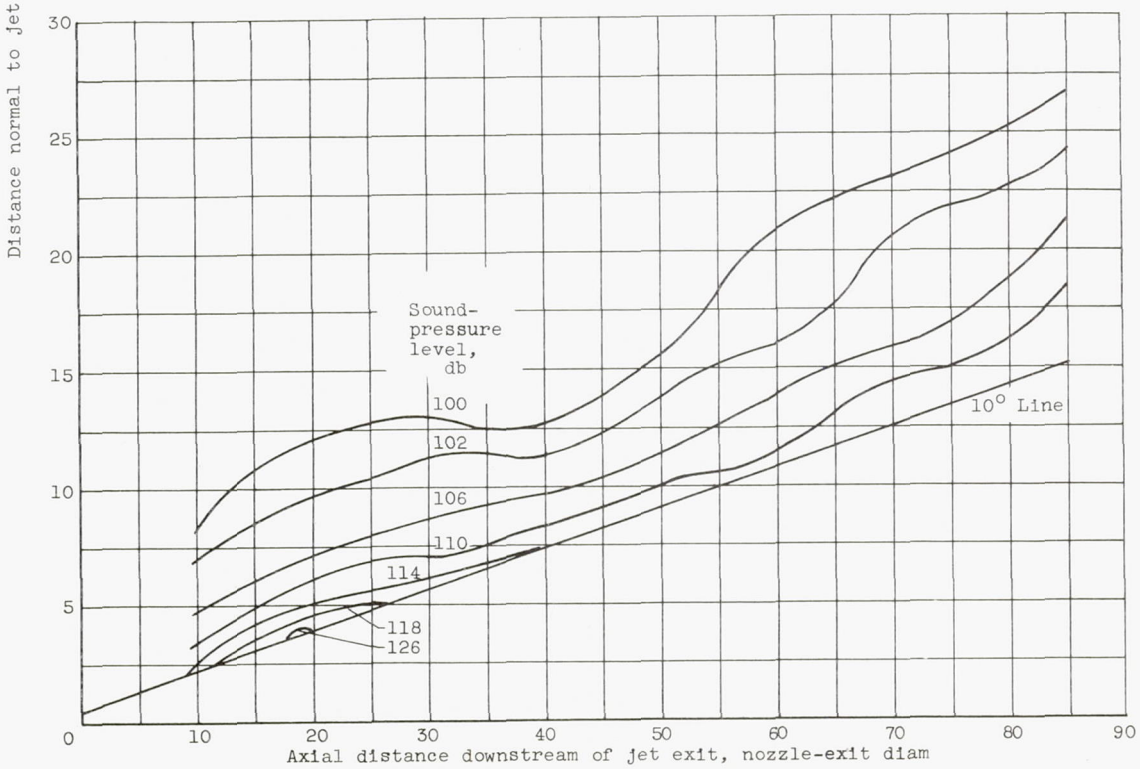

(b) Frequency band, 89 to 112 cycles per second.

Figure 10. - Near-field contours of noise from convergent nozzle.

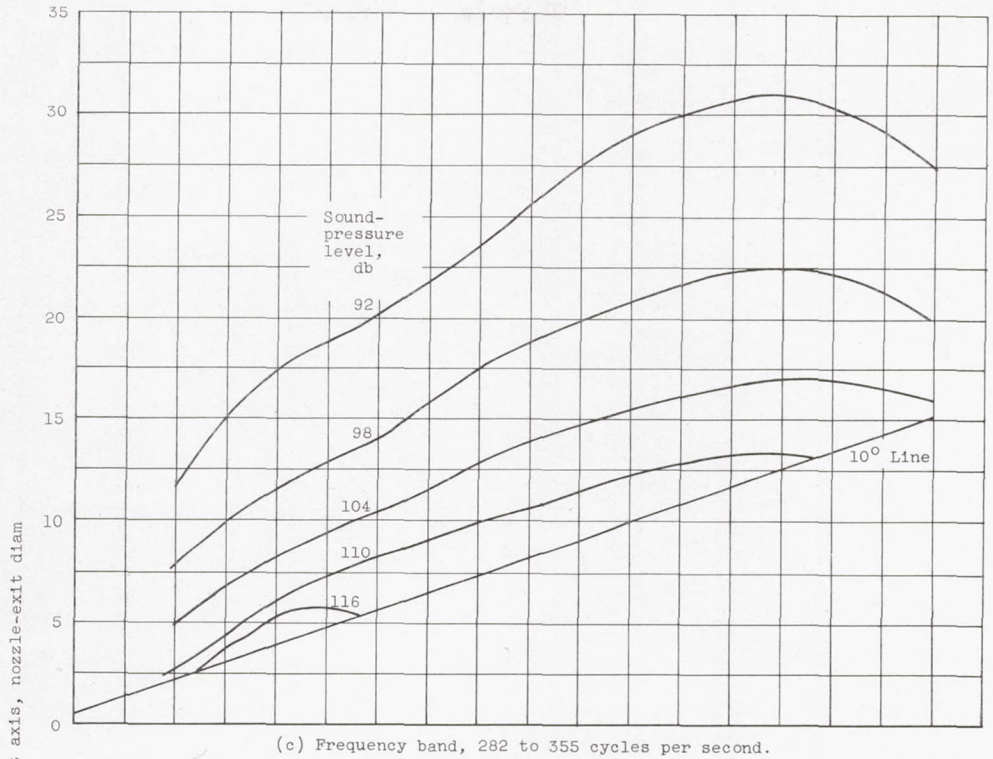

(c) Frequency band, 282 to 355 cycles per second.

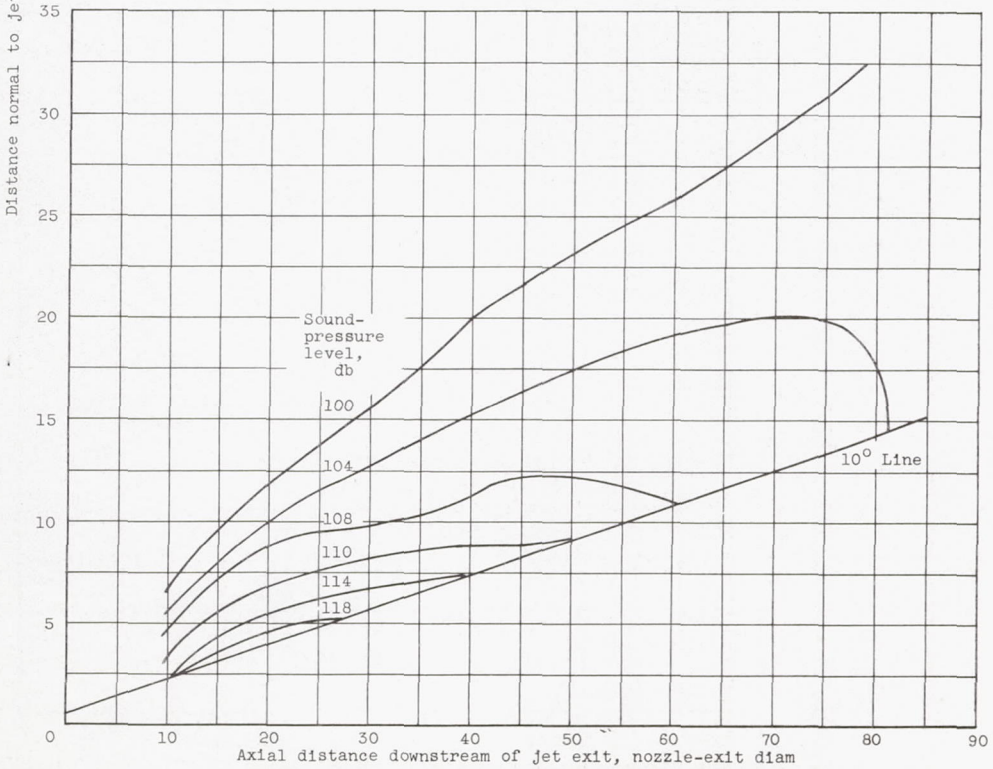

(d) Frequency band, 891 to 1120 cycles per second.

Figure 10. - Continued. Near-field contours of noise from convergent nozzle.

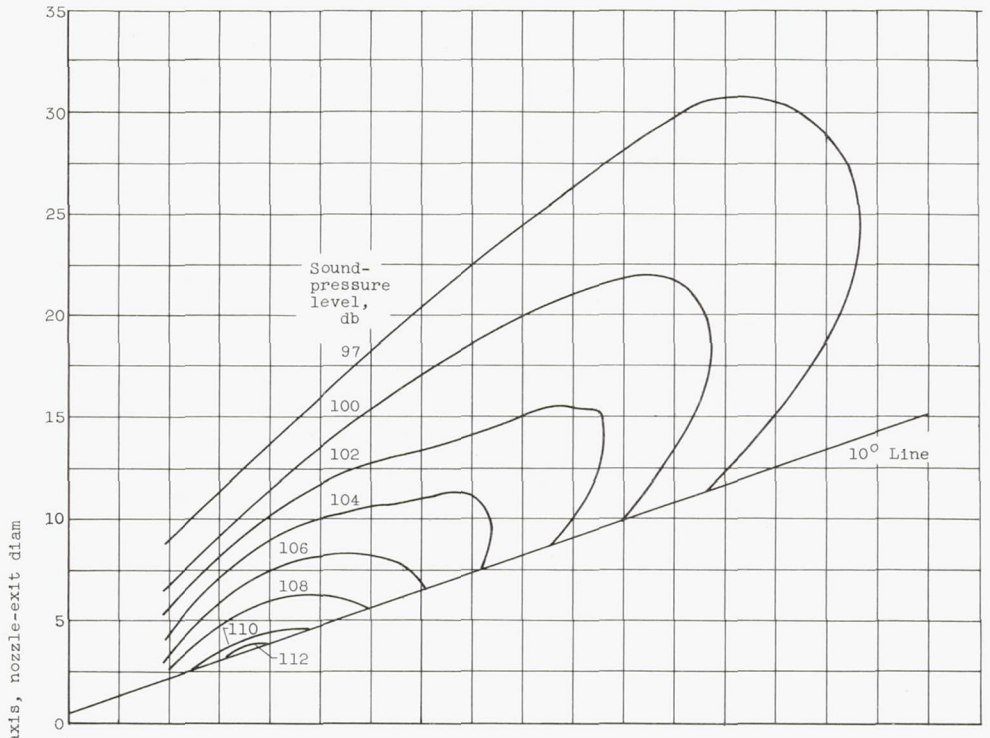

(e) Frequency band, 2820 to 3550 cycles per second.

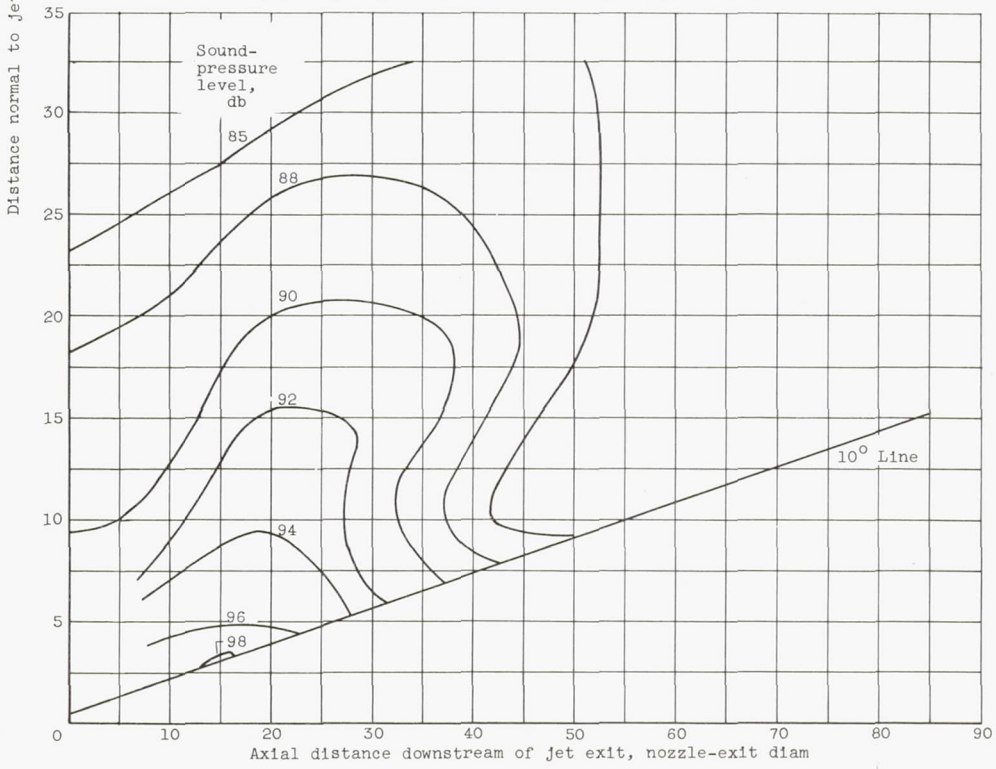

(f) Frequency band, 8910 to 11,200 cycles per second.

Figure 10. - Concluded. Near-field contours of noise from convergent nozzle.

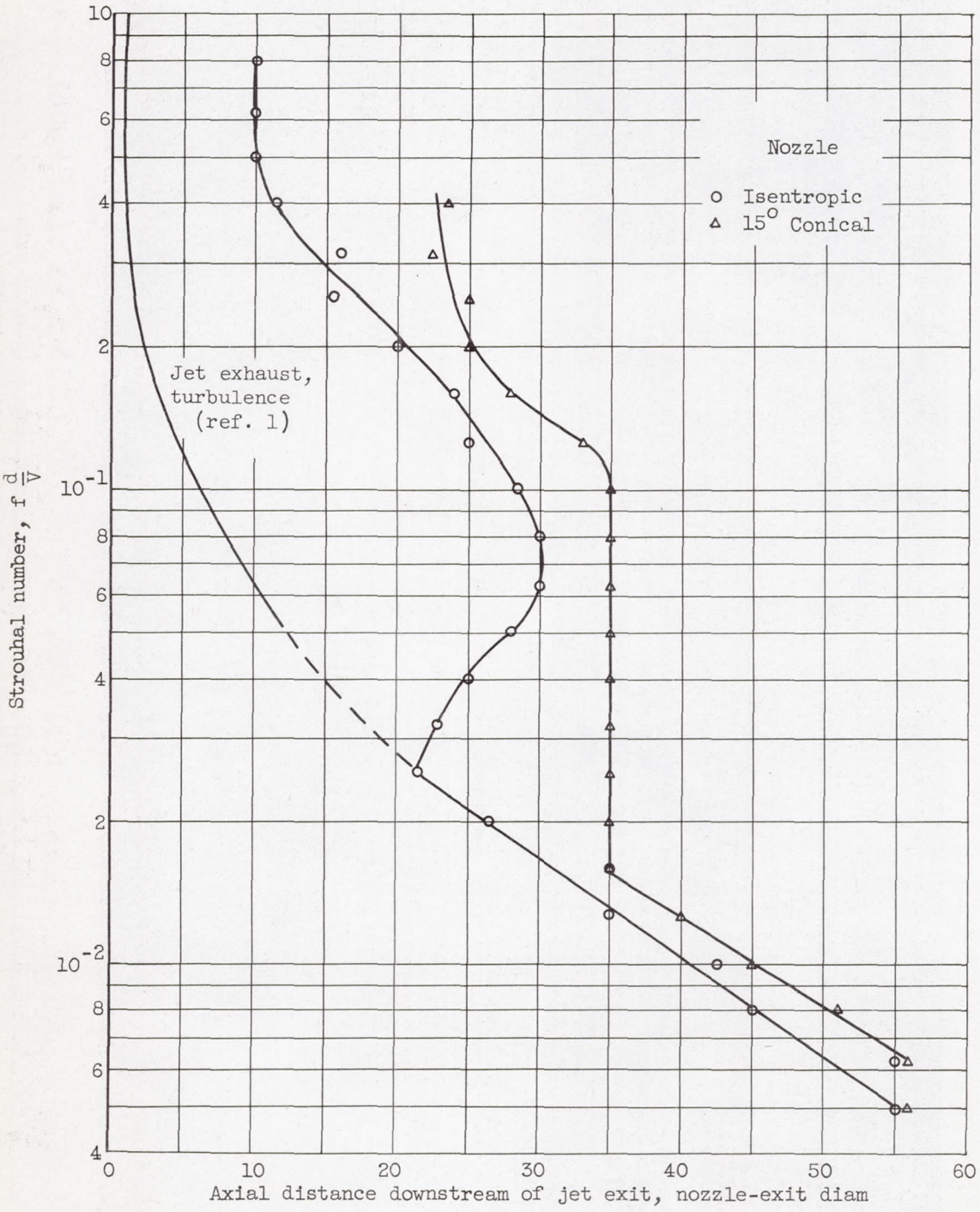

Figure 11. - Location of maximum pressure level for given Strouhal number in nozzle-exit diameters downstream of jet exit.

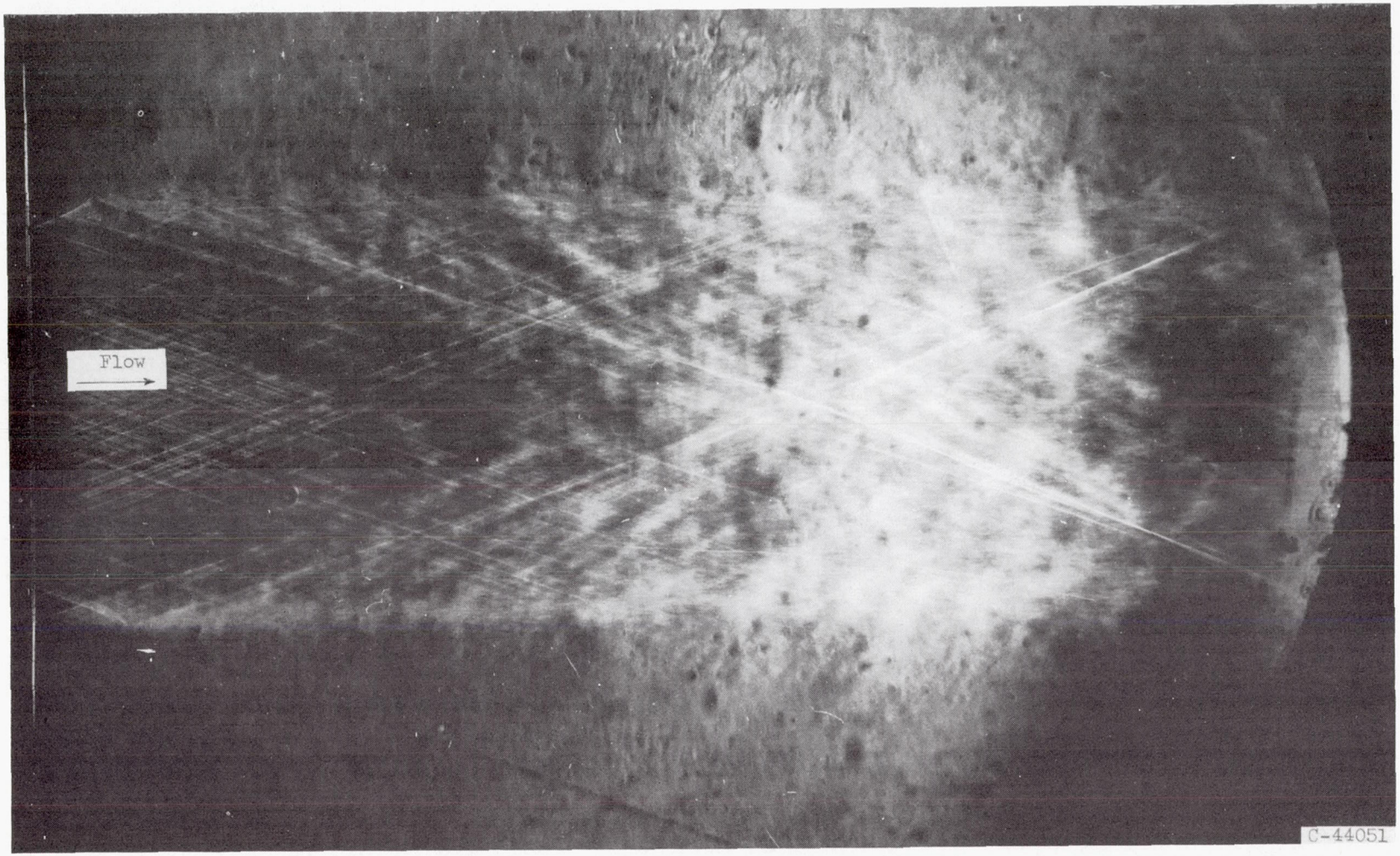

(a) Isentropic nozzle.

Figure 12. - Schlieren photographs of flow immediately downstream of nozzle exit.

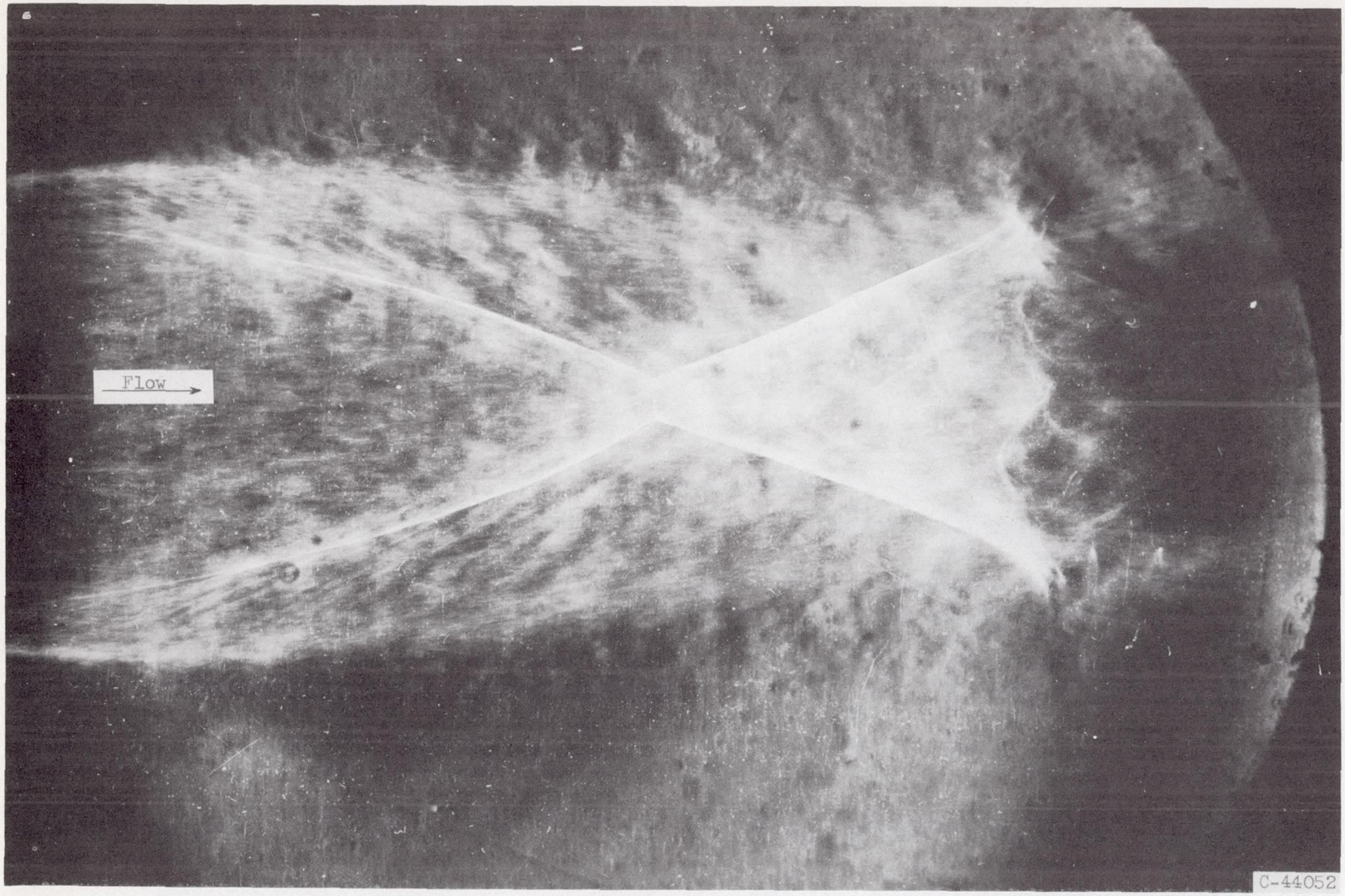

(b) Conical nozzle.

Figure 12. - Continued. Schlieren photographs of flow immediately downstream of nozzle exit.

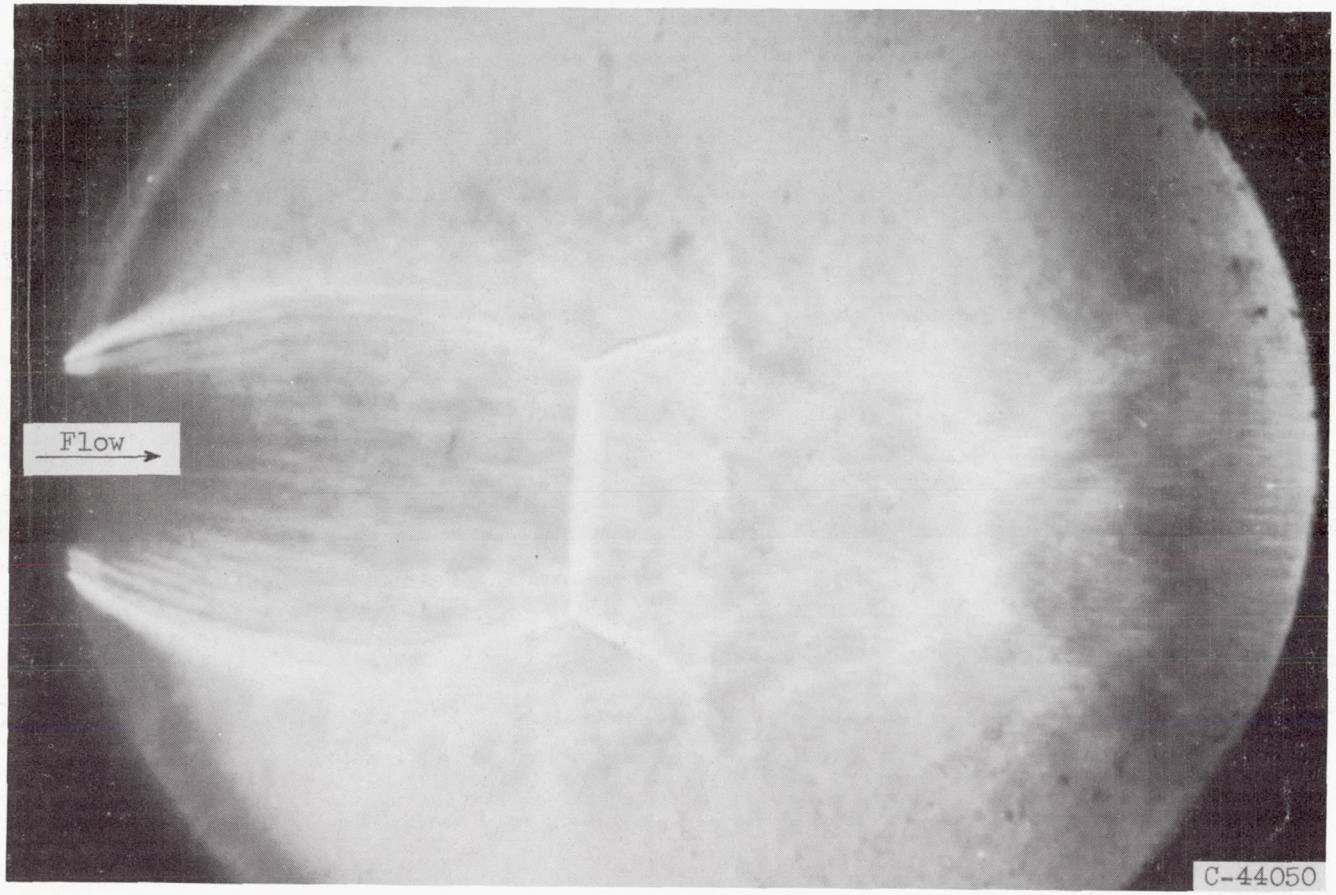

(c) Convergent nozzle.

Figure 12. - Concluded. Schlieren photographs of flow immediately downstream of nozzle exit.

NACA - Langley Field, Va.